Acta of Bioengineering and Biomechanics
Vol. 8, No. 1, 2006

Flow pattern and shear stress distribution in distal end-to-side anastomosis

JOSEF ADAMEC, JAN MATĚCHA, HANA NETŘEBSKÁ, JAN TŮMA

Czech Technical University in Prague,
Faculty of Mechanical Engineering, Department of Fluid Dynamics and Power Engineering,
Technická 4, Prague 6, 166 07, Czech Republic

We present the results of the first part of the project whose objective is to optimize the shape of anastomosis (end-to-side), which is used for the bypass anastomosis, and thus to minimize the negative impact of the flow dynamics on the vascular walls and blood, thanks to which the bypass failure risk can be successfully reduced. The Particle Image Velocimetry (PIV) method is used for experimental measurements that are combined with numerical solution. The goal of this work was to develop, both experimentally and numerically, a basic idea of flow behind the distal end-to-side bypass junction, depending on the connection angle both in steady and unsteady conditions.

Key words: anastomosis, bypass, flow dynamics, shear stress distribution

1. Introduction

In the research of human cardiovascular system, the understanding of hemodynamic characteristics of blood flow is indispensable. These characteristics have a decisive influence on studying destruction of blood elements and the damage to inner surface blood vessels. In our current civilization, diseases of the cardiovascular system are the major cause of mortality and morbidity among people in their productive age and among seniors. Bypassing is the most usual method allowing
a clogged or damaged artery to be bypassed with the material of a biological or synthetic type. In order to ensure long-term permeability of such a reconstruction, it is necessary to meet a number of conditions, including optimum hemodynamic characteristics of the reconstruction.
This project continues a set of previous projects, some for investigating unsteady flow by laser doppler anemometry (LDA) method [1]–[4], the others for using

particle image velocimetry (PIV) method, to investigate flow in cardiovascular models [5]–[7], etc.

2. Experiment

The experimental equipment (figure 1, left) for measurement by 2D PIV method in symmetry plane of bypass junction under steady conditions was constructed. The principle of PIV method is measuring the movement of the particles, which are added to the working fluid, during the known time interval. The bypass models were made from plexiglass with connection angles of 20°, 30°, 45°, 60° and 90°. The diameters of the host artery and graft were the same and equal to 10 mm. Solution of sodium iodide (58% NaI, ρ = 1730 kg/m^3, η = 0.00254 Ns/m^2, t = 24 °C) was used as a working fluid, because its refractive index is the same as refractive index of plexiglass and thus the optical distortions between the model and the working fluid were minimized.

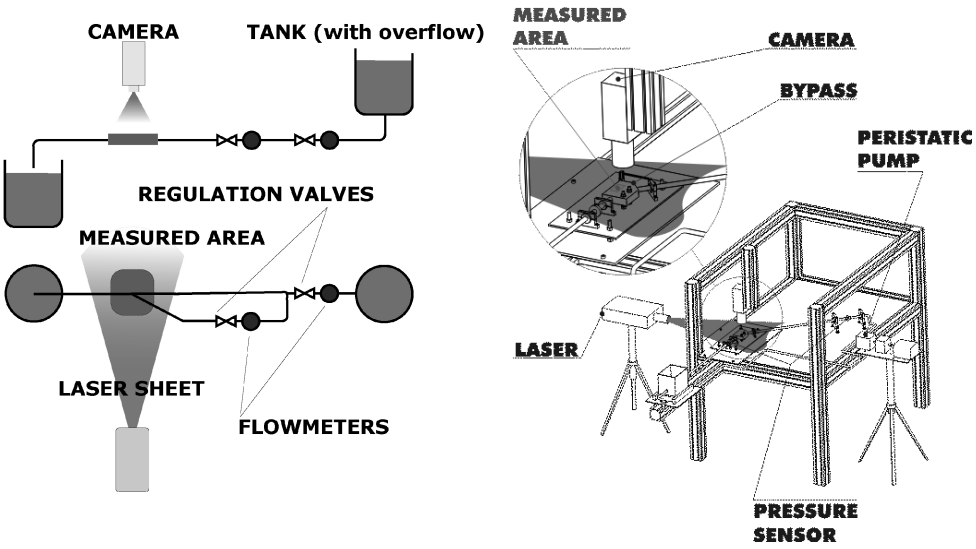

Fig. 1. Experimental equipment schemes. Left: for steady conditions, right: for unsteady conditions

Fluorescent particles with 1–20 μm diameters were used as seeding particles. The particles of this type were used because they allow filtering reflexes from laser on the boundary of the model and liquid. If these particles are illuminated with ND-YAG laser (l = 532 nm) and if the screen for camera (which transmits only the light with the wavelength greater than l = 580 nm) is used, then it is possible to scan only the light emitted from the particles and thus to filter out the reflections.

The flow field was measured in the symmetry plane of the model under steady conditions (Re = 500; 1400). Six areas (figure 2, left) were measured along the host artery (the length of the area measured was approximately 60 mm).
The experimental equipment (figure 1, right) for unsteady conditions that allows obtaining velocity flow field by PIV method in models of bypass junction in required instants of unsteady flow period and which allows synchronizing the flow field with data obtained from pressure transducers was designed and constructed. The flow fields were evaluated by commercial software which was extended with scripts in Matlab. These scripts, suggested in [8], enabled higher accuracy of flow field evaluation.

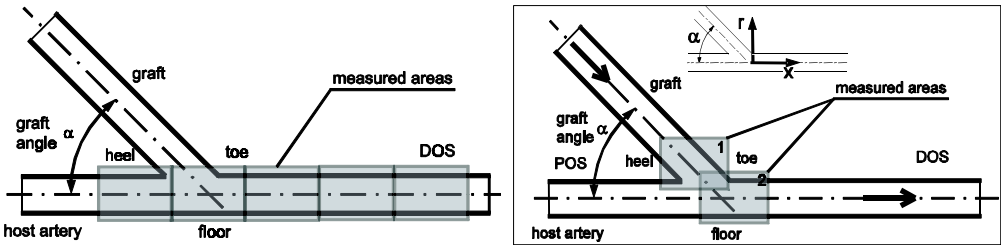

Fig. 2. Schemes of bypass. The areas measured by means of PIV
under steady conditions (on the left) and unsteady conditions (on the right)

The test circuit consisted of several parts. The peristaltic pump pumped the liquid from the tank to the model. One meter long pipe was placed before the model, and the pressure transducer was placed at the inlet end of the pipe. The second pipe was placed downstream the model. The liquid flowed from the model through the outflow pipe to the tank, and from the tank to the peristaltic pump. The peristaltic pump which ensured periodical unsteady flow was driven by stepping motor.

3. Numerical simulation

The numerical model geometry was derived from the geometry of the experiment and was slightly simplified against the experiment. The model consists of two tubes with inner diameter d = 10 mm. The length of graft to junction was 700 mm. The length of POS was 100 mm and it was closed in order to simulate the stenosis. The length of DOS was 700 mm. 3D computation grid was generated with hexahedron elements of about 800 000 cells. Simulations were performed for several models with different angle connection. Numerical simulations were calculated for Re = 500; 1400. The 58% solution of sodium iodide (NaI) was used as a working fluid. The solution was standarized to obtain a double precision segregated implicitly. The mathematical model was selected as the laminar model. The boundary conditions

were set on the input to the graft–velocity inlet, on the input to the host artery–wall and on the output–pressure outlet.

4. Results

The numerical models were created so that the developed laminar flow was in graft upstream junction place. The complex flow structures begin to create in the junction place.

The region of stream with maximum velocity, which is in graft in the center of the pipe due to developed laminar flow, is shown in figure 3, right. This stream divides along the symmetry plane after its impact on the wall (floor) and begins to climb up the sides of host artery and creates the external envelope of the flow. The flow is formed into two symmetric helixes (figures 3, 4).

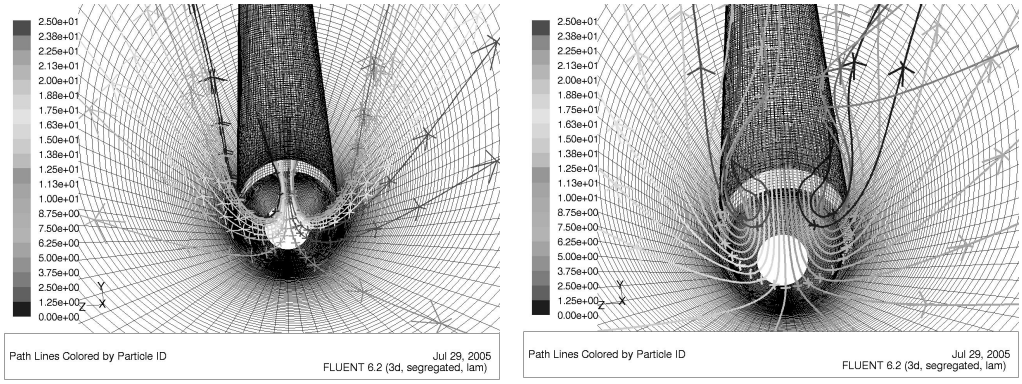

Fig. 3. The path lines from CFD under steady conditions.
The path lines from the area close to toe (left), the path lines from the center of graft (right)

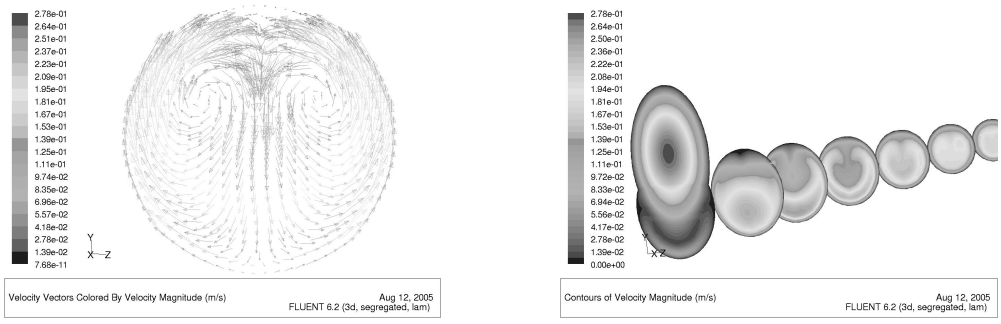

Fig. 4. The velocity field in bypass with connection angle of 45º under steady conditions (from CFD).
The flow field in cross-section in x = 10 mm (left), development of flow field (right)

The fluid from the slower stream (it is nearer the wall in the graft) gets into the center of this envelope. The fluid from region near the toe flows into host artery and begins to create two symmetric helical vortices in envelope of faster flow (figure 3, left). Small area with recirculation is formed in the region close to junction. This region is smaller at smaller graft angles until it disappears. The presence of this region was identified by experimental measurements, too.
Very small part of this flow returns in POS direction after impact on the floor and behind the input laminar flow creates vortex structure consisting of two vortices which rotate in reverse direction. The part of this flow returns to the main stream along the host artery sides.

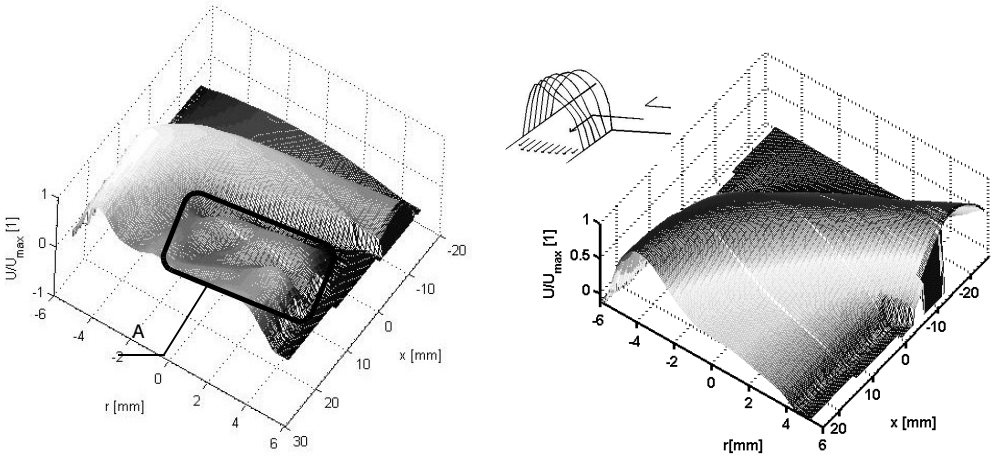

Fig. 5. Velocity distribution in *x* direction under steady conditions (from PIV):
at connection angle of 60º (left), at connection angle of 20º (right)

Good agreement between the experiments and numerical simulations of flow in bypass was shown by the velocity profile characteristics (figure 6, right). The deviation of these profiles in the symmetry plane can be caused by several factors. Inaccuracy of making models was due to milling and there was a problem with an alignment. This was responsible for different formation of the flow, especially different formation of the secondary flow.

It was difficult to use the pressure boundary condition because of a minimal difference in pressures. Therefore use was made of the velocity inlet boundary condition. The velocity in bypass was derived from the mass flow data measured. Because of ultrasound meter (which was used) accuracy some differences existed between experimental reality and the data measured.

The influence of the graft angle on flow field is given in figure 5 which shows the flow fields in symmetry plane measured by PIV. In the region of host artery (figure 5,

left A), the flow field in the host artery axis direction decreases monotonically at the small graft angle. The areas with higher and lower velocities appear in this region with increasing angle at the projection of flow field onto the symmetry plane. This is caused by an increase in the secondary flow with an increase in graft angle which can be seen from the numerical simulation.

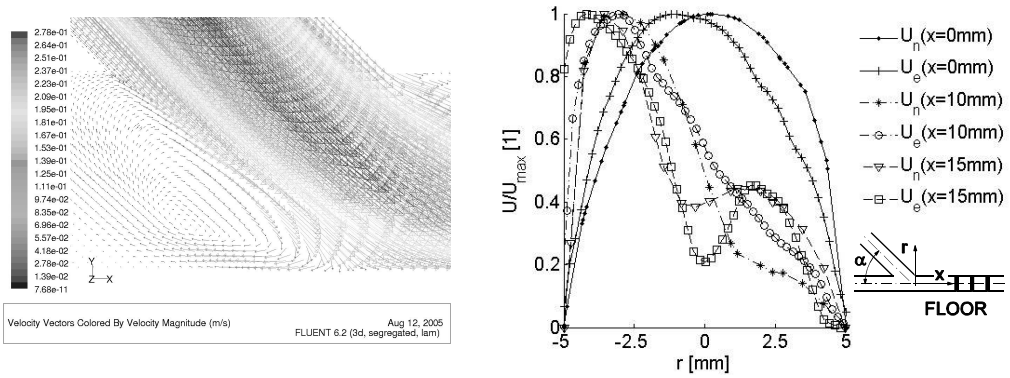

Fig. 6. Detail of vortex structure in POS direction at connection angle of 45° (from CFD) (left), comparison of experimental with numerical velocity profiles in several places at angle of 30° (right)

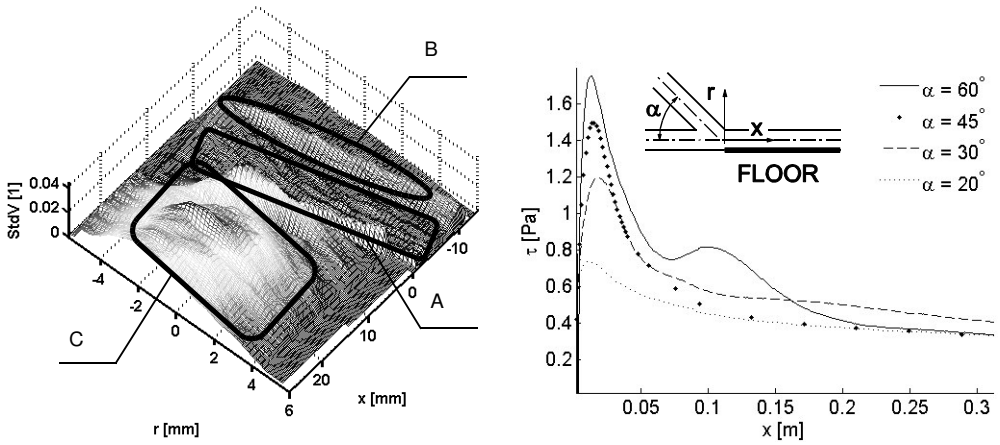

Fig. 7. Standard deviation of velocity in *x* direction at connection angle of 60° (PIV) (left), comparison of WSS on the floor for different angles (CFD) (right)

The next variable, i.e., the velocity fluctuations, is evaluated based on the data measured by PIV method. The area with minor fluctuations is in the region where the liquid flows from the graft into the host artery and further in graft direction (figure 7, left A). On the boundaries of this area there are areas with slightly increased

fluctuations (figure 7, left B). The area with the largest fluctuations is marked as C in figure 7. This area is featureless at smaller angles. The total value of fluctuations increases with an angle increase.

The behaviours of WSS evaluated from CFD in symmetry plane at different graft angles are shown in figure 7. The magnitude of WSS behind the graft junction rises. The maximum value of WSS is approximately at the distance of one diameter from the junction. It shifts downstream for greater graft angles and upstream for smaller graft angles. The maximum value of WSS increases with an increase in the graft angle. The behaviours of WSS for floor and opposite the floor are similar. For floor, maximum values are approximately three to four times bigger.

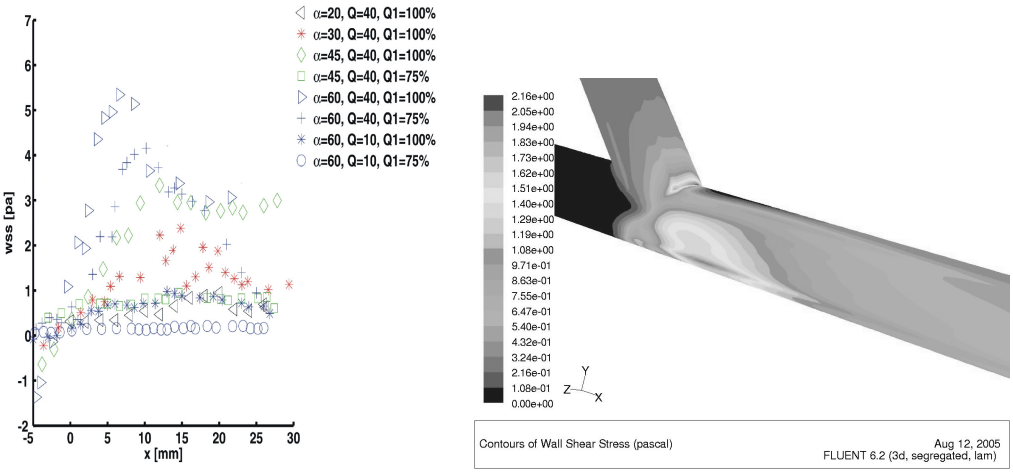

Fig. 8. Mean velocity gradients multiplied by dynamic viscosity at different graft angles and different flow regimes from PIV (left), wall shear stress at the angle of 45° from CFD (right)

The values of velocity profile gradient on the floor, multiplied by dynamic viscosity of working fluid, evaluated from PIV data, are shown in figure 8 for several models and several regimes measured. The behaviour of these values is similar to that of WSS evaluated from CFD. Figure 8 shows that the maximum value of WSS increases with an increase in the flow rate. If the flow rate in graft is 75% of the total flow rate, the maximum values of WSS decrease which can be seen in the behaviour of WSS at the angles 45° and 60°.

The unsteady periodic flow in the model of bypass anastomosis is very complex. The velocity profiles during the period in the host artery one diameter downstream the junction at graft angle $\alpha = 20°$ are seen in figure 9. The velocity profiles reach the maximum value near the floor for major part of the period. The velocity gradient which is connected with the wall shear stress is higher on the floor than on the opposite side. The second peak of velocity occurs near the side opposite the floor in some parts of the

cycle
which is caused by the secondary flow. The secondary flow is intensive in models with greater angle. Unlike the flow in steady conditions the greater vortex structures and reverse flow appeared especially in decelerating part of the cycle. The comparison of velocity filed between two angles for one instant of period is seen in figure 10. The magnitude of fluctuations varies during the period. The area with higher magnitude is downstream the junction. This area is bigger at greater angle. The maximum fluctuations observed near the wall are caused by worse signal.

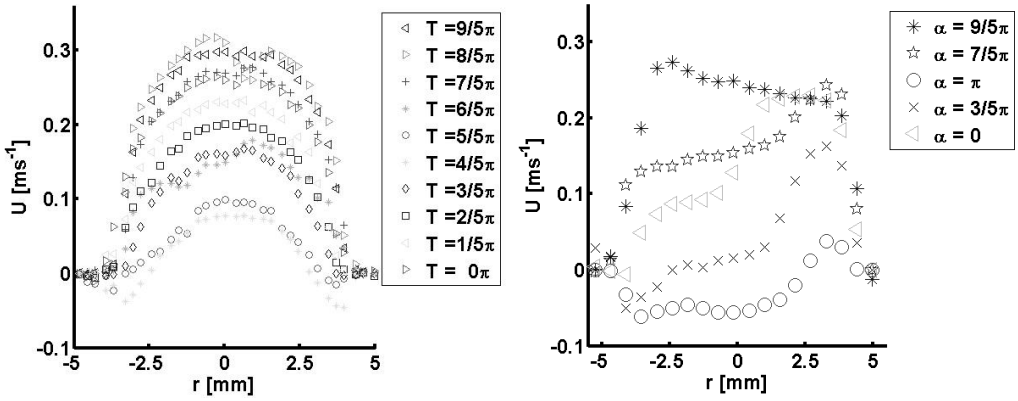

Fig. 9. Velocity profiles during the whole period in the graft one diameter upstream the junction (left), velocity profiles during the period in the host artery one diameter downstream the junction at graft angle of 20° (right)

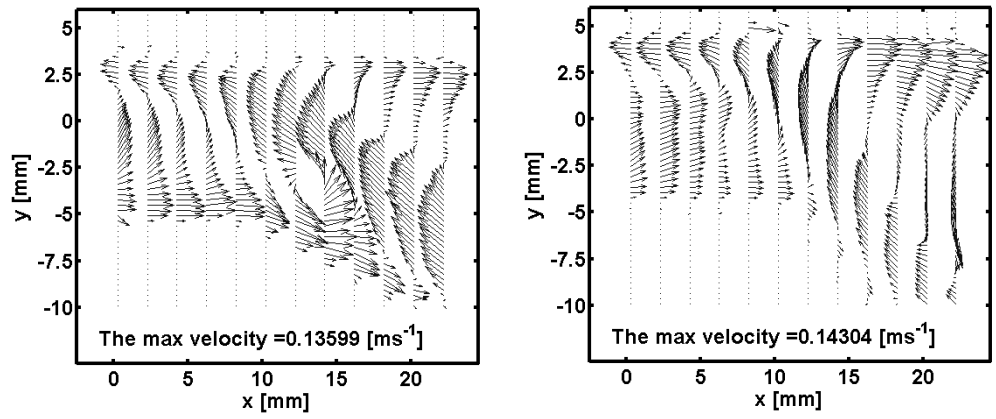

Fig. 10. Velocity profiles for the instant $T = 4/5\pi$ from PIV: at the graft angle of 20° (left), at the graft angle of 60° (right)

5. Conclusion

The flow field in bypass model was described based on the results from CFD and PIV. The velocity fields, fluctuation velocity fields at different angles of connection and different flow regimes were evaluated from PIV data. The behaviour of velocity profile gradients on the wall were evaluated. The influence of the connection angle on the velocity field and velocity fluctuation field was evaluated. The behaviour of WSS in the symmetry plane was evaluated from CFD calculations. Velocity profiles in the symmetry plane obtained from CFD and PIV data were compared. The agreement between the resultant flow characteristics obtained from CFD and the experiment showed that the type, location and selected accuracy of boundary conditions were appropriate. More perfect coincidence is assumed when using grid with more computation cells.

One of the problems when evaluating WSS is the velocity assessment near the wall. Near the wall the particles need not to follow the flow (e.g., the particles get stuck on the wall). When using PIV method the reflections of laser beam appear on the boundary between working fluid and the model. This problem was solved by using fluorescent particles and filter which transmits only the light whose wavelength l exceeds 580 nm. The gradient of velocity profile at the wall was evaluated as equivalent to WSS. The gradient was obtained by fitting a curve with several values of velocity measured near the wall. The results have corresponding qualitative character when compared with the results from CFD and even with the results which could be found in literature. The calibration measurement by CTA method is planned in order to verify the methodology of WSS evaluation by PIV method.

On the basis of the experiments performed and the experience gained, flow characteristics measurements of connection model by stereo PIV method for obtaining 3D flow field, the measurement at pulsated flow for obtaining flow field in the whole period, extending of bypass model with part with stenosis placed in the connection vicinity, are prepared.

Acknowledgements

This research has been supported by grant of GA ČR 101/05/0675 Theoretical and Experimental Optimalization of Vascular Reconstruction in the View of Hemodynamics.

References

[1] Adamec J., Nožička J., Kořenář J., *Turbulent Stress in Unsteady Fluid Flow*, Danubia-Adria Symposiumon Experimental Methods in Solid Mechanics – Abstracts, Warsaw, 2002, pp. 174–175.

[2] ADAMEC J., NOŽIČKA J., HANUS D., KOŘENÁŘ J., *Experimental Investigation of Pulsatile Flow in Circular Tubes*, Journal of Propulsion and Power, USA, 2001, Vol. 17, No. 5, pp. 1133–1136.

[3] ADAMEC J., NOŽIČKA J., KOŘENÁŘ J., *Reynolds Stress in Pulsatile Flow*, Danubia-Adria Symposium. Proceedings – Extended Summaries, Steyr: Austrian Society of Experimental Strain Analysis, 2001, pp. 135–136.

[4] ADAMEC J., NOŽIČKA J., KOŘENÁŘ J., *Investigation of the Pulsatile Pipe Flow*, International Journal of Heat and Technology, Italy, 2000, Vol. 18, No. 2, pp. 17–22.

[5] ADAMEC J., MATĚCHA J., NETŘEBSKÁ H., TŮMA J., *Flow Pattern and Shear Stress Distribution in Distal End-to-Side Anastomosis*, The 22nd Danubia-Adria Symposium on Experimental Methods in Solid Mechanics, Parma, 2005, pp. 86–87.

[6] MATĚCHA J., NETŘEBSKÁ H., TŮMA J., ADAMEC J., BÍCA M., *Flow Investigation behind the End-to-Side Anastomosis*, The 16-th International Symposium on Transport Phenomena, Prague, 2005, pp. 107.

[7] MATĚCHA J., NETŘEBSKÁ H., TŮMA J., SCHMIRLER M., ADAMEC J., *Unsteady Flow Investigation behind the End-to-Side Anastomosis*, The 3rd European Medical and Biological Engineering Conference, Prague, 2005.

[8] PĚTA M., NOVOTNÝ J., *Image Processing in PIV*, [in:] The 16-th International Symposium on Transport Phenomena, Praha, Czech Technical University in Prague, 2005, s. 140.

[9] CHUA L.P., YU S.C.M., TAM W.P., *PIV measurements of proximal models with different anastomotic angles*, Nanyang Technical University, Singapore. PII S0735-1933(00)00134-2.

[1] BATES C.J., O'DOHERTY D.M., WILLIAMS D., *Flow instabilities in a graft anastomosis: a study of the instantaneous velocity fields*, Proc. Instn. Mech. Engrs., 2001, Vol. 215, pp. 579–587,

[2] HEISE M., SCHMIDT S., KRÜGER U., RÜCKERT R., RÖSLER S., NEUHAUS P., SETTMACHER U., *Flow pattern and shear stress distribution of distal end-to-side anastomoses. A comparison of the instantaneous velocity fields obtained by particle image velocimetry*, Journal of Biomechanics, Vol. 37, No. 7, pp. 1043–1051.

[3] JACKSON Z.S., ISHIBASHI H., GOTLIEB A.I., LANGILLE B.L., *Effect of anastomotic angle on vascular tissue responses at end-to-side arterial grafts*, Journal of Vascular Surgery, August 2001, Vol. 31, No. 2, pp. 300–307.

[4] KEYNTON R.S., EVANCHO M.M., SIMS L.R., RITTGERS E.L., RODWAY N.V., GOBIN A., *Intimal Hyperplasia and Wall Shear in Arterial Bypass Graft Distal Anastomoses: An In Vivo Model Study*, Journal of Biomechanical Engineering, October 2001, Vol. 123, pp. 464–473.

[5] DEPLANO V., BERTOLOTTI V., BOIRON O., *Numerical Simulations of Unsteady Flows in a Stenosed Coronary Bypass Graft*, Medical & Biological Engineering & Computing, 2001, Vol. 9, pp. 488–499.